The almost mobility edge in the almost Mathieu equation

Yi Zhang, Daniel Bulmash, Akash V. Maharaj, Chao-Ming Jian, and Steven A. Kivelson
Department of Physics, Stanford University, Stanford, California 94305, USA
(Dated: June 29, 2015)

Harper's equation (aka the "almost Mathieu" equation) famously describes the quantum dynamics of an electron on a one dimensional lattice in the presence of an incommensurate potential with magnitude V and wave number Q. It has been proven that all states are delocalized if V is less than a critical value $V_c = 2t$ and localized if $V > V_c$. Here, we show that this result (while correct) is highly misleading, at least in the small Q limit. In particular, for $V < V_c$ there is an abrupt crossover akin to a mobility edge at an energy E_c; states with energy $|E| < E_c$ are robustly delocalized, but those in the tails of the density of states, with $|E| > E_c$, form a set of narrow bands with exponentially small bandwidths $\sim t\ \exp[-(2\pi\alpha/Q)]$ (where α is an energy dependent number of order 1) separated by band-gaps $\sim tQ$. Thus, the states with $|E| > E_c$ are "almost localized" in that they have an exponentially large effective mass and are easily localized by small perturbations. We establish this both using exact numerical solution of the problem, and by exploiting the well known fact that the same eigenvalue problem arises in the Hofstadter problem of an electron moving on a 2D lattice in the presence of a magnetic field, $B = Q/2\pi$. From the 2D perspective, the almost localized states are simply the Landau levels associated with semiclassical precession around closed contours of constant quasiparticle energy; that they are not truly localized reflects an extremely subtle form of magnetic breakdown.

I. INTRODUCTION

Quasiperiodic ordered states of matter possess two or more periodic structures whose periods are incommensurate with each other. Examples of such materials include quasicrystals and crystals with incommensurate charge or spin density waves as well as simple crystals in the presence of a generic uniform magnetic field. The absence of even discrete translational symmetry fundamentally distinguishes quasiperiodic from crystalline (periodic) structures. The absence of quenched randomness makes them conceptually distinct from disordered systems, although because in both cases Bloch's theorem does not apply, there is no requirement that the elementary excitations are delocalized.

As one of the simplest examples in the family, Aubry and Andre studied in 1980 the following one-dimensional finite-difference Schrodinger equation with a quasiperiodic potential[1]

$$t\,(f_{n+1} + f_{n-1}) + V\cos(Qn + \theta)\, f_n = E\, f_n \tag{1}$$

where $n \in \mathbb{Z}$ labels discrete sites, t is the nearest neighbor hopping amplitude, V and Q are the amplitude and wave vector of the incommensurate potential ($Q/2\pi \in (0,1)$ is irrational), and $-\theta/Q$ defines an "origin" of the incommensurate potential. Without loss of generality, we use the convention in which $V > 0$, $t > 0$ and open boundary conditions for a finite size system. This eigenvalue equation is generally referred to in the physics literature as Harper's equation or the Aubry-Andre equation and in the mathematics literature as the "almost Mathieu equation" (an analogy with the continuous Mathieu equation). We will use the name Harper's equation from here on.

Clearly, this is the eigenvalue equation corresponding to a one-dimensional tight-binding Hamiltonian in the presence of a quasiperiodic potential, which in second-quantized representation is

$$H_{1D} = \sum_n \left[t\left(c^\dagger_{n+1}c_n + c^\dagger_{n-1}c_n\right) + V\cos(Qn+\theta)\, c^\dagger_n c_n \right] \tag{2}$$

where E is an energy eigenvalue and $\alpha^\dagger = \sum_n f_n c^\dagger_n$ is the creation operator for the corresponding eigenstate. The same eigenvalue equation arises in the "Hofstadter problem" of an electron moving in a two-dimensional square lattice in the presence of a magnetic field corresponding to $Q/2\pi$ flux quanta per plaquette.

There is a well-known self-duality in Harper's equation[1–3] which interchanges the roles of the kinetic and potential energy terms, $V/2 \leftrightarrow t$. Specifically, in terms of Fourier transformed variables,

$$\begin{aligned} f_n &= \frac{\exp(i\phi n)}{\sqrt{L}} \sum_m g_m \exp(imnQ + i\theta m) \\ g_m &= \frac{\exp(-i\theta m)}{\sqrt{L}} \sum_n f_n \exp(-imnQ - i\phi n) \end{aligned} \tag{3}$$

where L is the system size. It is easy to see that g_m satisfies the dual Harper's equation

$$\frac{V}{2}\,(g_{m+1} + g_{m-1}) + 2t\cos(Qm + \varphi)\, g_m = E g_m. \tag{4}$$

This equation is self-dual when $V = 2t$.

The spectrum and transport properties of this system have been extensively studied for over thirty years, in a wide set of contexts in mathematics and statistical mechanics. In particular, the solution of the "Ten Martini Problem"[4,5] proves that the spectrum is a Cantor set for $V \neq 0$ and arbitrary "incommensurate" Q, *i.e.* so long as $Q/2\pi$ is irrational. There has also been progress towards experimental realization in cold atom systems[6]. It is widely believed[1–3,7,8] that for any Q that is incommensurate, there is a *single* "metal-insulator" transition at the self-dual point, $V = 2t$, such that the spectrum is absolutely continuous and all eigenstates are de-localized for $V < 2t$, while the spectrum is pure-point and all eigenstates are localized for $V > 2t$. The same line of reasoning leads to the conclusion that the spectrum is singularly continuous and the eigenstates are 'critical' for $V = 2t$.

In this paper, we revisit Harper's equation from various perspectives. We show that a conventional semiclassical analysis of the associated Hofstadter problem suggests that for a weak potential, $V < 2t$, and small $Q/2\pi \ll 1$, there exist two mobility edges at $E_{c,\pm} = \pm|2t - V|$ that separate the localized states with $E < E_{c,-}$ and $E > E_{c,+}$, from the delocalized states with $E_{c,-} < E < E_{c,+}$; *i.e.*, the states near the band edges are effectively localized even for a weak incommensurate potential. This conclusion is apparently verified by "exact" numerical studies, even when eigenenergies are computed with an accuracy exceeding 1 part in 10^{12}. The resolution of this apparent contradiction comes from a calculable breakdown of the semiclassical analysis, and a careful analysis of the numerics; while the states outside the apparent mobility edges are, in fact, delocalized, they form exponentially narrow bands – essentially Landau levels – with correspondingly large effective masses, $m^* \sim t^{-1}\exp[(2\alpha\pi/Q)]$, where α is a dimensionless function of $|E - E_c|$ and $V/2t$. While these states are technically delocalized, for even moderately small $Q/2\pi$ they are so weakly dispersing that for all physical purposes they behave as if localized; we refer to these as "almost localized" states, understanding the physics of which is one of the main results of the paper. Moreover, a similar analysis in the case $V > 2t$, still with $Q/2\pi \ll 1$, reveals that there is a hidden "almost transition" characterized by the emergence of a real-space Fermi surface. For large wave vector $Q/2\pi \sim O(1)$ and relatively small potential V, we find that perturbation theory gives a satisfactory characterization and results in a series of gaps in the spectrum, whose sizes and locations are determined by the values of V/t and Q; all states are robustly de-localized.

The rest of the paper is organized as follows. In Sec. II, we study the physical properties of Harper's equation in the limit where $Q \ll 2\pi$, analytically using a semiclassical approximation and by numerical methods, which suggests the existence of two mobility edges. In particular, because the system is one dimensional, we are able to employ an extremely efficient recursive method to obtain numerical solutions for extremely large system sizes, even with lengths in excess of 10^6 sites, so we have been able to test the validity of all our analytic arguments with great precision. In Sec. III, we consider high-order perturbations and show that it reconciles the conflict between Sec. II and previous phase diagram. Especially, we characterize the essential properties of the states near the band edges and why the conclusions of Sec. II is physically relevant. In Sec. IV we discuss the previously overlooked "transition" as a function of energy that occurs when $Q \ll 2\pi$ and $V > 2t$, even though all the states are robustly localized. In Sec. V, we briefly present our theoretical understanding and numerical results for the situation in which the wave vector $Q \sim O(1)$. We conclude and discuss relations with previous work in Sec. VI.

II. LONG PERIOD INCOMMENSURATE ORDER, $Q \ll 2\pi$

In this section we present semiclassical and numerical studies concerning the spectral and transport properties of Harper's equation when the period of the incommensurate potential is large in units of the lattice constant.

	Open along k_x	Closed	Open along k_y
$V > 2t$	$\|E\| < V - 2t$	$\|E\| > V - 2t$	N.A.
$V < 2t$	N.A.	$\|E\| > 2t - V$	$\|E\| < 2t - V$
$V = 2t$	$E = 0$	$E \neq 0$	$E = 0$

TABLE I: Topologies of the constant energy contours. See Fig. 1 for illustrations. Note that for $V = 2t$ and $E = 0$ the contour is a perfect square and connected along both the k_x and k_y directions at isolated points $(\pi, 0)$ and $(0, \pi)$.

A. Semiclassical theory of a 2D crystal in a magnetic field

It is well known that Harper's equation also describes the Hofstadter problem - a model of a two-dimensional (2D) crystal in the presence of an *incommensurate* magnetic flux density. To establish such an equivalence, consider a 2D tight-binding model on a square lattice with hopping matrix element t along the $\hat{x}$ direction and $V/2$ along the $\hat{y}$ direction and with an effective magnetic field $\vec{B} = B\hat{z}$ where $B = Q/2\pi$ so that there are $Q/2\pi$ magnetic flux quanta per plaquette. In a gauge chosen to preserve translation symmetry along the $\hat{y}$ direction, so that the Bloch wave-number k_y is a conserved quantity, the Hamiltonian is

$$H_{2D} = \sum_{n,k_y}\left[t\left(c^\dagger_{n+1,k_y}c_{n,k_y} + \text{H.C.}\right) + V\cos\left(Qn + k_y\right)c^\dagger_{n,k_y}c_{n,k_y}\right] \tag{5}$$

where n is the lattice distance along the $\hat{x}$ direction. Thus, in the subspace of fixed k_y, with the identification $\theta \leftrightarrow k_y$ and leaving the k_y index implicit $c_{n,k_y} \to c_n$, the Hofstadter problem problem is seen to be identical to Harper's equation in Eq. 2. Moreover, in the thermodynamic limit, when $Q/2\pi$ is irrational, spatially averaged physical quantities such as the density of states (DOS) and the localization length are independent of k_y for the same reason that they are independent of the origin of coordinates (θ) of an incommensurate potential. (See Ref. 10 and Appendix A for more detailed discussions.) Thus, the summation over k_y in Eq. 5 only produces a degeneracy factor of L_y.

Alternatively, we can choose the gauge that preserves translation symmetry along the $\hat{x}$ direction:

$$H_{2D'} = \sum_{m,k_x}\left[\frac{V}{2}\left(c^\dagger_{m+1,k_x}c_{m,k_x} + \text{H.C.}\right) + 2t\cos\left(k_x - Qm\right)c^\dagger_{m,k_x}c_{m,k_x}\right] \tag{6}$$

where m and k_x label the lattice site and momentum along the $\hat{y}$ and $\hat{x}$ directions, respectively. In this gauge, $H_{2D'}$ is equivalent to the dual form of Harper's equation in Eq. 4. The duality is thus identified with two different gauge choices for the Hofstadter problem.

We can study the localization properties of the one-dimensional crystal with an incommensurate potential by considering whether the eigenstates of the corresponding two-dimensional crystal in a magnetic field are localized along

the $\hat{x}$ direction, which is the spatial direction in the original one-dimensional problem[10]. When the "field strength" $B = Q/2\pi \ll 1$, the dynamics of Bloch electrons is given semiclassically by the Lorentz force law:

$$\hbar \frac{d\vec{k}}{dt} = -e\vec{v}(\vec{k}) \times \vec{B} = \frac{e}{\hbar}\left(\vec{B} \times \frac{dE(\vec{k})}{d\vec{k}}\right) \tag{7}$$

where $\vec{v}(\vec{k}) = \frac{dE(\vec{k})}{\hbar d\vec{k}}$ is the electron group velocity. The resulting electron orbits in two-dimensional momentum space are confined to constant energy contours determined by the zero-field energy dispersion $E = \epsilon_k = 2t\cos k_x + V\cos k_y$. Since the velocity of an electron is perpendicular to the constant energy contour, the semiclassical motion is localized in the $\hat{x}$ direction unless the contour is open along the k_y direction, which occurs when $V < 2t - |E|$. (See Table I for the parameter regimes for different topologies of the Fermi surface and Fig. 1 for illustrations.) This seemingly implies that for potential amplitude $V < 2t$ there are two mobility edges at $E_{c,\pm} = \pm(2t - V)$; the states are de-localized between these energies, while all states beyond the mobility edges are localized. (For $V > 2t$ the same analysis leads to the conclusion that all states are localized.) If we start from a pristine one-dimensional crystal and slowly turn on V, the states near the band edges localize first, and as V increases the energy window of de-localization between the two putative mobility edges becomes smaller and eventually closes at $V = 2t$. This is in sharp contrast to the expectation that all states are de-localized for $V < 2t$.

The wave vector Q in Harper's equation plays the role of a magnetic field in the two-dimensional crystal scenario. For $B = Q/2\pi \ll 1$, the semiclassical results are expected to be asymptotically exact, and the transition should thus be almost independent of Q. (Exceptions can arise when $V \ll 2t$ or $V \gg 2t$ where the strong anisotropy and curvature of the 2D constant energy contours invalidates the semiclassical approximation, as will be discussed further in Sec. III.) For larger Q, however, the magnetic field can induce tunneling between separate semiclassical orbits, a phenomenon known as magnetic breakdown[11]. In particular, for $Q \sim O(1)$ there is no reason to trust the semiclassical theory at all, so for the purposes of the present section, we limit ourselves to small Q and will only return to consider $Q \sim O(1)$ in Sec. V.

To test the validity of our semiclassical arguments, we will now discuss numerical studies of the localization length and the density of states (DOS).

B. Numerical results

Since the one-dimensional Hamiltonian can be written as a tri-diagonal matrix, numerical calculations are efficient with recursive methods even for large system sizes[10]. In particular, we calculate the two-point Green's function $G(n,n') = (E + i\delta - H)^{-1}_{n,n'}$. If the states are localized at energy E, then the Green's function should be exponentially decaying with the distance between the two points $G(n,n') \propto$

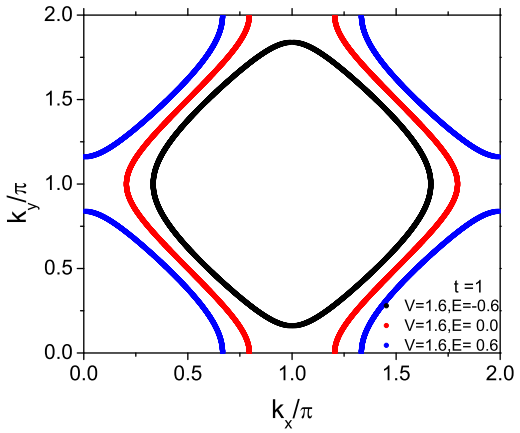

(a)

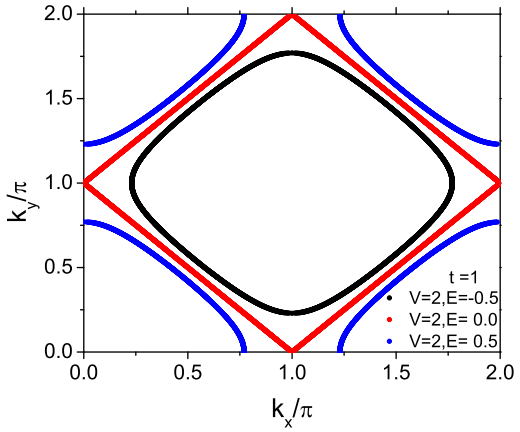

(b)

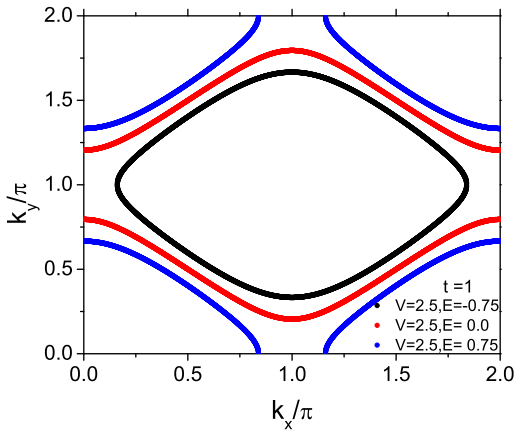

(c)

FIG. 1: Constant energy contours (a) for $V < 2t$, (b) at the self-dual point, $V = 2t$, and (c) for $V > 2t$. The black curves are at $E < -|2t - V|$, the red at $E = 0$, and blue at $E > |2t - V|$. The black and blue curves are closed contours while the red one is open in different directions for different V and is at the Lifshitz transition when $V = 2t$. Note that $t = 1.0$, $V = 2.5$ and $t = 0.8$, $V = 2$ are equivalent up to an energy rescaling: $E \to 0.8E$.

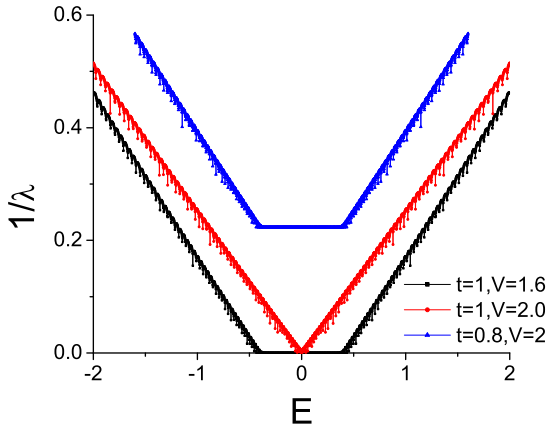

FIG. 2: The inverse localization length $1/\lambda$ as a function of energy for three different parameter regimes at $Q = 1/31$. The system size is $L = 7.2 \times 10^5$. The blue and black curves are related by the duality transformation in Eq. 3 connecting the Hamiltonians in Eqs. 1 and 4. The localization length is always finite for the blue curve, for which $V > 2t$ and corresponds to the constant energy contours in Fig. 1(c). However, there is a portion of the spectrum that is apparently delocalized for the black curve, for which $V < 2t$ corresponding to the constant energy contours in Fig. 1(a). The red curve at the self-dual point $V = 2t$ corresponds to the contours in Fig. 1(b).

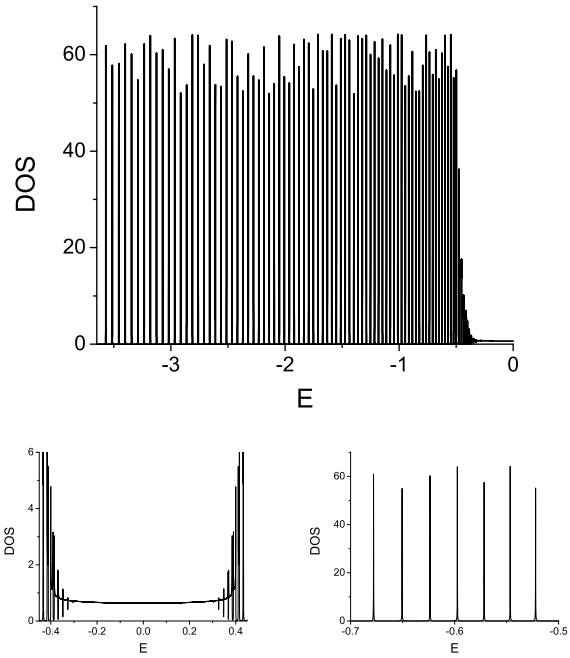

FIG. 3: The DOS $\rho(E)$ of Harper's equation with parameters $t = 1$, $V = 1.6$ and $Q = 1/31$. The system size is $L = 7.2 \times 10^5$ and $\delta = 0.0001$ brings in a small but finite energy resolution. Drastically different behaviors are observed above and below $E = \pm 0.4$. Note that the spectrum is particle-hole symmetric therefore only the $E < 0$ half is shown. In practice, it is obtained through the computation for the dual Harper's equation with $t = 0.8$, $V = 2$ and $Q = 1/31$. The lower panels are regimes between and just beyond the apparent mobility edges on an expanded scale, another expansion near the band edge is shown in Fig. 5.

$\exp(-|n-n'|/\lambda)$ where λ is the localization length; otherwise the system is delocalized and $\lambda \to \infty$ ($1/\lambda \to 0$). In all cases we have carried out calculations on systems of sizes L large enough that the results are independent of L - which often means up to sizes $L \sim 10^6$ sites.

We study the localization properties for a representative small $Q = 1/31 = 2\pi(1/62\pi) \sim 2\pi(5.1 \times 10^{-3})$ and for various values of t, V, and E that lead to different topologies of the associated two-dimensional constant energy contours as shown in Fig. 1. In Fig. 2 we display the results of numerical studies of the inverse localization length as a function of E for various values of V/t. The results are consistent with the inferences made in the previous section on the basis of the two-dimensional semiclassical theory: if the energy contour is closed (black and blue curves in Figs. 1(a)-1(c)) or open along the k_x direction (red in Fig. 1(c)), the corresponding states in the one-dimensional (1D) problem are localized. If the energy contour is open along the k_y direction (red in Fig. 1(a)), the 1D states are delocalized. In particular, for $V < 2t$ but $|E| > 2t - V$ the results indicate that the states are localized – consistent with expectations from semiclassical theory but in conflict with previous claims[1–3,7,8].

We have also computed the density of states (DOS) at energy E, defined as $\rho(E) = -\frac{1}{\pi L}\sum_n \mathrm{Im}G(n,n)$, using the same methods[10]. Our algorithm is most efficient and accurate when the system is localized and the Green's function is exponentially suppressed. However, even if the parameters to be considered are in the de-localized regime, the spectral properties are the same as those of the dual Harper's equation given in Eq. 4, which is necessarily localized[18]. For this reason, where the states are delocalized, we always compute the DOS from the localized dual.

An example of the sort of DOS so obtained is shown in Fig. 3 for $t = 1$,$V = 1.6$ and $Q = 1/31$. Drastically different behaviors are observed above and below $E = \pm 0.4$. For $|E| > 0.4$, there are discrete sharp peaks separated by resolvable gaps while for $0.4 > |E|$, the DOS appears to be a smoothly varying function of E. The correspondence with the semiclassical treatment of the 2D version is that the discrete peaks correspond to Landau levels where the constant energy contours (at zero field) are closed. The continuous spectrum arises where the energy contours are open, and the apparent mobility edges correspond to the Lifshitz transitions at which the topology of these contours changes (see Table I).

More generally, Fig. 4 is the phase diagram of Harper's equation with $Q = 1/31$ extracted from localization length calculations. The phase boundaries for $V < 2t$ and $V > 2t$ are colored in black and red, respectively, and are fully consistent with $E_c = \pm(2t - V)$ (blue lines) derived from the semiclassical treatment of the 2D model, as given in Table I. On the $V < 2t$ side of the phase diagram, an apparent metal insulator transition produces qualitative changes in both the localization length λ and the DOS ρ. On the $V > 2t$ side, however,

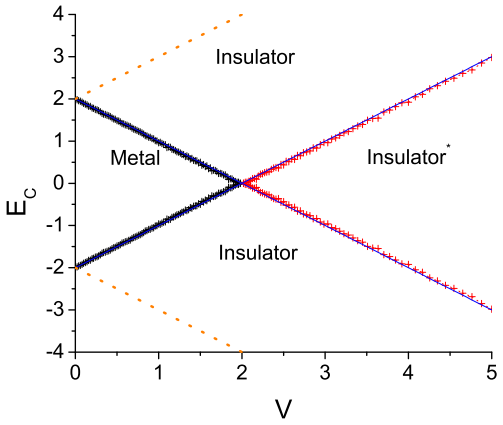

FIG. 4: The phase diagram for Harper's equation with $t = 1$ and $Q = 1/31$ obtained from numerical study of localization length on a system of size $L = 7.2 \times 10^5$. For each $V < 2t$, E_c (black) separates the regimes of metal (localization length $\lambda \to \infty$) and insulator (*i.e.* with available numerical accuracy, λ is finite). For $V > 2$, the critical values of E_c (red) are obtained by a duality transformation of the $V < 2t$ cases. Change of DOS behaviors is observed on both $V < 2t$ and $V > 2t$ phase boundaries, though on both sides of the latter phase boundary the system is localized and insulating. The blue solid lines are $E_c = \pm(2t - V)$ in accord with Table I. The orange dotted lines are the band edges at $E = \pm(2t + V)$. One important caveat is that there is an implicit energy resolution on the level of machine precision in our numerical calculations. For infinite precision, the phase diagram will essentially reduce to a single metal-insulator transition at $V = 2t$, see Sec. III for more details.

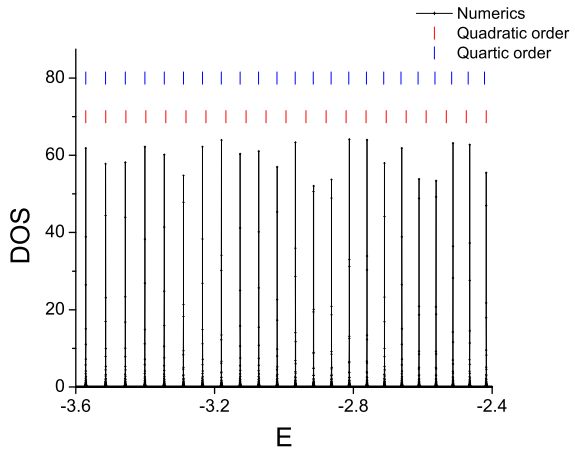

FIG. 5: The DOS $\rho(E)$ with the same parameters $t = 1$, $V = 1.6$, $\delta = 0.0001$, and $Q = 1/31$ as in Fig. 3, near the lower band edge but on an expanded scale.. The red and blue marks on the top label the locations of the discrete Landau levels from the expansions of the electron dispersion to quadratic order (free-electron approximation) and quartic order in momentum, respectively.

while the analogous change in the structure of the DOS seemingly signifies the existence of a transition (the dual of the metal-insulator transition) the localization length is finite on both sides of the transition. We will discuss the nature of this "insulator-insulator" transition in Sec. IV.

C. Localization near the band edges from the 2D perspective

It is easy to prove that the spectrum of Harper's equation is confined to the range of energies $|E| \le 2t + V$. One important qualitative point that is less obvious is that the states near the lower band edge $E \sim -2t - V$ (and the upper band edge, $E \sim 2t+V$) always appear localized, whether or not V is larger than $2t$. This is most easily understood from the 2D perspective, H_{2D} in Eq. 5. In the absence of an effective magnetic field ($Q/2\pi = 0$), the dispersion near the band-bottom is accurately treated in the effective mass approximation, which means that for small but non-zero Q, the low energy spectrum is well approximated as Landau levels. This accounts both for the discrete peaks in the spectrum and their spatial localization.

To be specific, we expand the zero-field energy dispersion of H_{2D} to quadratic order of k around the band minimum at (π, π):

$$\epsilon_k = 2t\cos k_x + V\cos k_y \approx -2t - V + tq_x^2 + \frac{V}{2}q_y^2 + \dots \quad (8)$$

where $(q_x, q_y) = (k_x, k_y) - (\pi, \pi)$. The effective magnetic field is $Q/2\pi$ flux quanta per plaquette, and the corresponding effective cyclotron frequency is $\omega_C = Q\sqrt{2tV}$. Thus, the energy levels near the lower band edge are quantized in Landau levels with $\epsilon_n \approx -2t - V + (n + 1/2)\omega_C$ where $n = 0,\ 1,\ 2,\ \cdots$. We show in Fig. 5 an enlargement of the DOS near the lower band edge obtained from numerical solution of H_{1D} with $t = 1$, $V = 1.6$, and $Q = 1/31$ as in Fig. 3; the corresponding values of ϵ_n are indicated by the red marks at the top of the figure.

The consistency is remarkable for the few lowest energy levels, where the effective mass approximation is highly accurate; at somewhat higher energy, however, while the energy levels remain sharp and gapped, the level spacing gradually decreases. However, the accuracy of the theoretical estimates can be improved by taking into account the higher order terms in the expansion of the energy dispersion, ϵ_k, e.g. $V\cos k_y \approx -V + \frac{V}{2}q_y^2 - \frac{V}{24}q_y^4 + O(q_y^6)$. The Landau level problem including the quartic terms is discussed in Appendix B, and the results (obtained with minimal numerical work[10]) are shown as the blue marks at the top of Fig. 5. This accounts quite accurately for the positions of the peaks in the DOS over the entire range of energies shown in the figure. The spatial extent of the wave-functions is determined by the effective magnetic length, $\ell \propto Q^{-1/2}$, which also determines the relevant range of momenta $\Delta k \sim 1/\ell$. Thus, the validity of the expansion in powers of k, and hence the validity of the Landau level analysis, relies both on the smallness of Q and on E being close to the band edge, $\omega_C \ll 4t$ and $|E + 2t + V| \ll 4t$. However, *at this level of approximation*, no aspect of the analysis is sensitive to whether or not V is larger or smaller than $2t$ (as long as the Landau level spacing ω_C is much smaller than the original band width, which requires $(Q/2\pi)^2 \ll V/2t \ll (2\pi/Q)^2$). We will focus more carefully on the properties of these band-edge states in Sec. III.

Closer to the band center, the fact that there is a periodic lattice qualitatively affects the Hofstadter problem. As required by duality, the resulting change from closed to open topology of the constant energy contours that occurs at $E = \pm E_c$ produces similar changes in the character of the DOS for $V < 2t$ or $V > 2t$. For $V < 2t$, there appears to be a continuous DOS for $|E| < E_c$ and the states are delocalized in the $\hat{x}$ direction, so in terms of the properties of the original 1D problem, E_c acts as a mobility edge in the traditional sense. However, for $V > 2t$, from the perspective of the original 1D problem, the states are robustly localized both above and below E_c; the nature of the crossover that occurs at $E = \pm E_c$ in this case will be discussed in Sec. IV.

III. RESOLVING THE PARADOX - DELOCALIZATION OF THE STATES NEAR THE BAND EDGES

As we have shown in Sec. II, the semiclassical and numerical results disagree qualitatively with the previous literature concerning both the localization and spectral properties of Harper's equation for small $Q \ll 2\pi$. In this section, we first briefly summarize the previous arguments that there is a single energy independent metal-insulator transition at $V = 2t$, and then examine more carefully the properties of the states near the band edges where the contradiction arises. In particular, we focus on two perturbations that have been neglected in the semiclassical approximation and show how they affect the localization problem. We will see, for $Q \ll 2\pi$ and $V < 2t$, the states near the band edges behave 'almost localized': even though their wavefunctions are extended, their bandwidth are exponentially small in $1/Q$, therefore they are easily localized in the presence of small perturbation or finite energy resolution.

A. Previous arguments on the localization transition

First of all, we briefly summarize the previous arguments[1,2]. In the notation of Eq. 3, we define

$$f(x) = \frac{\exp(i\phi x)}{\sqrt{L}} \sum_m g_m \exp\left(imQx + i\theta m\right) \tag{9}$$

as an extension of f_n, $n \in \mathbb{Z}$ to $x \in \mathbb{R}$. Since m takes integer values, for a g_m which remains normalizable in the $L \to \infty$ limit (that is, g is localized), $f(x)$ is a Bloch function with a fundamental period of $2\pi/Q$. Then the wavefunction f_n, though no longer periodic, is still extended due to its periodic envelope $f(x)$. Namely, if the solution to one specific Harper's equation is localized, its dual is necessarily extended.

We can further use the fact that the inverse localization length is related to the DOS through the Thouless formula:

$$1/\lambda(E) = \int dE' \ln\left|(E - E')/t\right| \rho(E') \tag{10}$$

which can be equally applied to the dual system in Eq. 4 with the same DOS ρ:

$$1/\lambda'(E) = \int dE' \ln\left|2(E - E')/V\right| \rho(E') \tag{11}$$

then $1/\lambda(E) = 1/\lambda'(E) + \ln(V/2t)$. This relation holds well as can be seen in Fig. 2: the Harper's equations corresponding to the blue and black curves are dual, and indeed there is a constant vertical shift of $\ln(V/2t)$ between them.

Let us first consider the case where states in the original system are localized: its dual is extended so $1/\lambda'(E) = 0$, therefore $1/\lambda(E) = \ln(V/2t) > 0$ is constrained to $V > 2t$. Similarly, if the original system is extended $1/\lambda(E) = 0$, its dual $1/\lambda'(E) = \ln(2t/V) > 0$ requires $V < 2t$. Consequently, all states are localized at all energy levels E for $V > 2t$, and all states are extended at all energy levels E for $V < 2t$.

There is an obvious contradiction between this argument and the two-dimensional semiclassical problem, where the duality corresponds to switching the roles of $\hat{x}$ and $\hat{y}$. For open constant energy contours (red and blue curves in Figs. 1(a) and 1(c)), the semiclassical theory does suggest that the system is either localized along $\hat{x}$ and de-localized along $\hat{y}$, or localized along $\hat{y}$ and de-localized along $\hat{x}$. However, there is a third possibility that the constant energy contour can be closed (black curves in Figs. 1(a) and 1(c)), where the states are physically localized along both the $\hat{x}$ and $\hat{y}$ directions. More specifically, while the previous claim that all states are localized for $V > 2t$ and the states between the two apparent mobility edges, i.e. those with $E_c = \pm(2t - V)$ are de-localized for $V < 2t$ is consistent with the results in Sec. II, both the semiclassical theory and the numerics seemingly imply that the states beyond the mobility edges at $\pm E \in (2t - V, 2t + V)$ are localized even for $V < 2t$.

B. Localization near the band edges from a real-space perspective

In Sec. II C, and more generally in Sec. II A, we found that the states near the lower band edge form effective Landau levels; at this level of approximation, the states in a Landau-level are exactly degenerate, and thus it is possible to construct eigenstates that are either localized or delocalized. In this circumstance, even parametrically small terms that are omitted can, in principle, play a qualitative role in resolving this degeneracy. In this subsection we consider the states near the lower band edge from a 1D real-space perspective, treating $Q \ll 2\pi$ as a small parameter. In particular, we show that exponentially small terms, $\sim \exp[-(2\alpha\pi/Q)]$ lift this degeneracy in such a way that the band-edge states are delocalized for $V < 2t$ and localized for $V > 2t$. Note that terms that produce these behaviors are so small for even moderate values of $2\pi/Q$ that they are entirely unobservable in the numerical studies of Sec. II B, despite their being carried out to less than 1 part in 10^{12} uncertainty! Conversely, since it is difficult to imagine circumstances in which the energy uncertainty (due to thermal broadening if nothing else) is anywhere near this small, this observation carries with it the implication that *for*

all plausible physical purposes, these states are effectively localized. It is in this sense that they are "almost localized."

Consider the states within a quantized energy level ϵ_n and the corresponding Hilbert subspace consisting of a single localized state per potential well consisting of $2\pi/Q$ sites. There are two perturbations that are exponentially small in $1/Q$ and implicitly neglected in the semiclassical theory in Sec. II – the tunneling between the potential wells $t_{\rm eff}$ and the local energy variation between the potential wells $V_{\rm eff}$, which turn out to be the key to resolving the conflicting conclusions. The way this occurs can be most easily seen from a simple variational analysis of the band-bottom states in the limit $Q \ll 1$.

Local energy difference between wells: To begin with, we construct a variational state centered near a single minimum of V of the gaussian form

$$f_n = \mathcal{N} e^{i\pi n} \exp[-(n-a)^2/2\ell^2] \tag{12}$$

where $\mathcal{N}$ is the normalization constant, while the center of localization, a, and the localization length, ℓ, are treated as variational parameters, although we will assume (and then confirm) that $2\pi/Q \gg \ell \gg 1$. The variational energy in this state is easily seen to be (using the Poisson summation formula)

$$\langle H \rangle = V \cos(Qa) e^{-Q^2\ell^2/4} - 2te^{-1/4\ell^2} + \delta E \tag{13}$$

where δE is all terms of order $e^{-\pi^2 m^2 \ell^2}$ with integer $m \geq 1$. Clearly, the leading order terms (ignoring δE) simply reproduce the results of the harmonic approximation in Eq. 8. The result is $a = \pi(1+2m)/Q$, $\ell = (2t/V)^{1/4}\sqrt{1/Q}$ giving a variational energy $\epsilon_0 \approx -2t - V + Q\sqrt{2tV}/2$ that is independent of m, *i.e.* the minimum of the potential in which it is localized.

This result is not exact. The leading contribution to its corrections can be readily seen by looking at the leading m dependent term in δE: $\delta E = -2Ve^{-\pi^2\ell^2}\cos(2\pi a) + \ldots$ where $\ldots$ refers to other terms of the same order which are independent of a, as well as higher order terms in powers of $e^{-\pi^2\ell^2}$. Thus, we see that there is an exponentially small difference in energy

$$V_{\rm eff} \sim V \exp[-\pi^2\ell^2] \tag{14}$$

between a state localized near $a = \pi/Q$ and the neighboring well at $a = 3\pi/Q$.

Tunneling between the potential wells: Using the same variational wavefunctions, we can readily estimate the tunneling matrix element between two neighboring states by simply evaluating the matrix element of the tunneling term in the Hamiltonian between localized states centered at $a = \pi/Q$ and $a = 3\pi/Q$. The result is

$$t_{\rm eff} \sim t \exp[-\pi^2/Q^2\ell^2]. \tag{15}$$

this is qualitatively consistent with the more careful analysis included in Appendix C.

From this simple variational treatment, we conclude that $V_{\rm eff} \gg t_{\rm eff}$ (*i.e.* the states are localized) so long as $Q^2\ell^4 < 1$, and conversely, that $V_{\rm eff} \ll t_{\rm eff}$ if $Q^2\ell^4 > 1$. Miraculously (and probably accidentally), since this variational approach yields $Q^2\ell^4 = 2t/V$, it reproduces the exact criterion for localization. (Note that in terms of parametric dependence on Q, $\ell^2 \sim Q^{-1/2}$, which implies that both ℓ^{-2} and $Q^2\ell^2$ are small compared to 1 when $Q \ll 1$, as promised.)

C. Localization near the band edge from the perspective of magnetic breakdown

To locate the localization transition more accurately, we consider related corrections to the 2D semiclassical theory from Sec. II A. So long as the effective magnetic field, $Q/2\pi$, is non-zero, the semiclassical theory is not exact, and in particular there is always a non-zero amplitude for magnetic breakdown across the Brillouin zone boundaries. While the amplitude for such processes is exponentially small, they are exactly the terms that determine whether the states in a given Landau level are localized or not.

Magnetic breakdown along the $\hat{y}$ and $\hat{x}$ directions produce essentially different outcomes: the former results in an open constant energy contour along the $\hat{y}$ direction and hence delocalization along the $\hat{x}$ direction, and thus is associated with $t_{\rm eff}$; the latter results in an open constant energy contour along the $\hat{x}$ direction and hence is associated with local energy differences in potential wells, $V_{\rm eff}$. Manifestly, when $V > 2t$, the constant energy contour near the band edge is anisotropic and elongated along the $\hat{x}$ direction, and conversely for $V < 2t$. (See Fig. 1.) Therefore magnetic breakdown occurs predominantly along the $\hat{x}$, so that the states are localized suggesting $V_{\rm eff} > 2t_{\rm eff}$, or $\hat{y}$ direction so that the states are de-localized suggesting $V_{\rm eff} < 2t_{\rm eff}$, depending on whether $V/2t$ is greater or less than 1. Indeed, the constant energy contours are symmetric under $\pi/2$ rotation only at the self-dual point of $V = 2t$, which means that only here is $V_{\rm eff}/2t_{\rm eff} = 1$. A further implication of this is that the spectrum forms a Cantor set, since for each Landau band of the original problem, *i.e.* for each value of the energy level ϵ_n, the effective Hamiltonian confined to the space of states spanned by this Landau level defines a new version of Harper's equation, but with much smaller energy scale and longer length scale. These results are indeed consistent with previous conclusions[1–3,7,8].

D. Numerical tests for "moderate" $Q/2\pi$

To test this perspective, we numerically exact diagonalize Harper's equation Hamiltonian for a representative value of $Q = 1/5$, which is still small compared to 2π, but not so small that exponentially small effects are beyond the realm of numerical studies (even by setting $\delta = 0$). We take $L = 377 \approx 12\,(2\pi/Q)$, the probability distribution of some lowest eigenstates for $t = 1$ and $V = 1.6$ (upper panel) or $V = 2.5$ (lower panel) are shown in Fig. 6. We can clearly see that the states near the lower band edge are localized for $V = 2.5t > 2t$ but clearly extended for $V = 1.6t < 2t$ – once we can resolve the exponentially small perturbations.

We note that similar arguments can be useful for the identification of the metal-insulator transition and mobility edges in

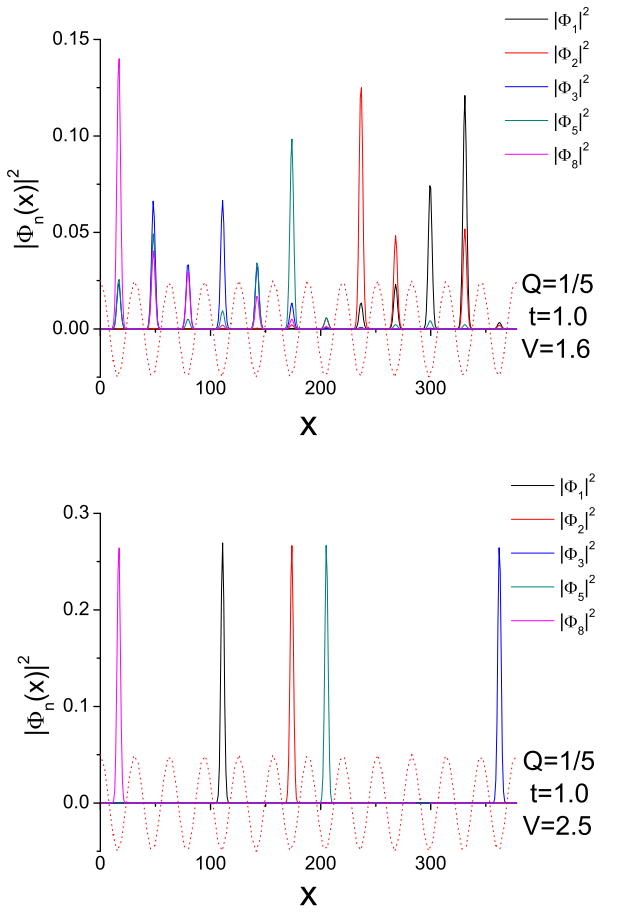

FIG. 6: The probability amplitude of lowest eigenstates of Harper's equation for $Q = 1/5$, $t = 1$, $V = 1.6$ (upper panel) and $V = 2.5$ (lower panel). The results are obtained through exact diagonalization on system size $L = 377 \approx 12\,(2\pi/Q)$ with almost 12 complete potential wells. The dotted red curves are illustrations of the $V\cos(Qx)$ potential profile (not to scale).

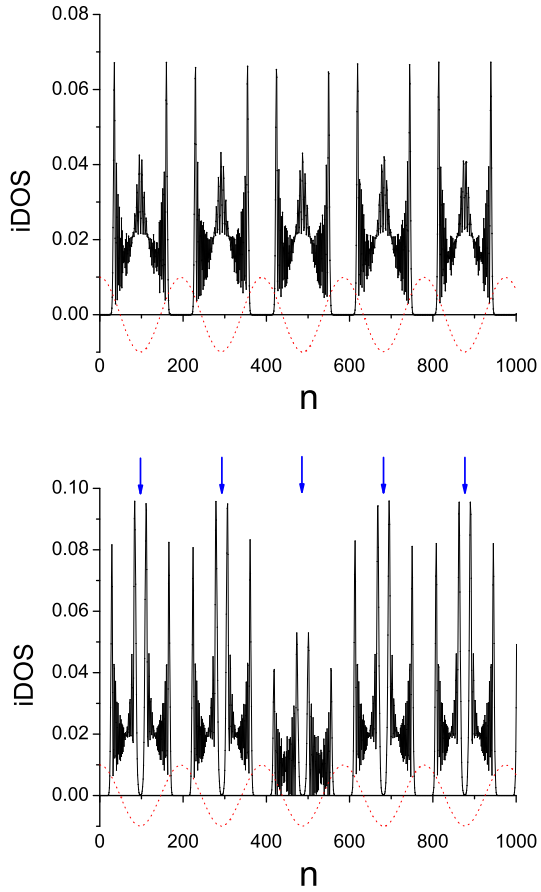

FIG. 7: The local electron integrated DOS of Harper's equation $\int_{E_{min}}^{E_{max}} dE\,|f_n(E)|^2$ with $t = 1$, $V = 2.5$ and $Q = 1/31$ for states within the energy range $-0.8 < E < -0.7$ (upper panel) and $-0.4 < E < -0.3$ (lower panel), respectively. The red dotted curve is an illustration of the incommensurate periodic potential (not to scale). The blue arrows in the lower panel mark additional dips appearing at the potential minima.

the generalized versions of Harper's equations such as the examples considered in Ref. 9, where one can simply compare the quantum tunneling amplitudes across the $\hat{x}$ and $\hat{y}$ directions in the equivalent two-dimensional Hofstadter's problem. Further details and examples are included in Appendix D.

IV. HIDDEN CROSSOVER FOR $V > 2t$ AND $Q \ll 2\pi$: A REAL-SPACE FERMI SURFACE

In the previous sections, we have discussed the effective metal-insulator transition for Harper's equation with $V < 2t$ and $Q \ll 2\pi$, where drastically different behaviors of the spectral and transport properties are observed in the physical limit on the two sides of the apparent mobility edges $\pm E_c = 2t - V$. In the current section, let us turn to the related 'insulator-insulator' transition at $\pm E_c = V - 2t$ in the duality transformed systems for $V > 2t$ and $Q \ll 2\pi$, see Fig. 4. All states are localized for $V > 2t$, yet the behavior of the DOS still shows a sharp change in character at E_c, see Fig. 3. What is the nature of this transition?

First of all, the Pauli exclusion principle forbids the electron density per site exceeding one. As we have shown in Sec. II, near the band edges the electron eigenstates of Harper's equation localized in each potential well resembles that of a harmonic oscillator with their electron density mostly concentrated around the potential minima. Heuristically, for a deep potential well, the electron density there will reach one electron per site after filling a finite number of quantized levels. For $Q \ll 2\pi$ the potential around the minima is slow varying, therefore the nearby lattice sites have a band width approximately equal to $W = 4t$ – the band width of an infinite 1D chain with $V = 0$. From the lower band edge $E = -2t - V$, these sites will reach maximum electron density at $E = 2t - V$ consistent with E_c if $V > 2t$.

For illustration, we calculate the local electron integrated DOS of Harper's equation within an energy range

$\int_{E_{min}}^{E_{max}} dE\,|f_n(E)|^2$ with $t = 1$, $V = 2.5$ and $Q = 1/31$, and the results are shown in Fig. 7 for the energy ranges $-0.8 < E < -0.7$ (upper panel) and $-0.4 < E < -0.3$ (lower panel) corresponding to the two respective insulating phases in Fig. 4. Characteristic dips in the local electron density at the potential minima are clearly present as marked by the blue arrows in the lower panel, a signal that the electron density there has reached maximum below $E = -0.4$. These dips broaden as energy E increases and more sites reach maximum electron density. Consequently, for Fermi energy E_F between $\pm E_c$, the real-space electron density after filling all states below E_F receives non-analytic singularities when it drops from maximally filled to partially filled - similar to the momentum-space electron density of a metal at the Fermi surface but in the real space instead. The real-space electron density $\int_{-2t-V}^{E_F} dE\,|f_n(E)|^2$ for all states below the Fermi energy E_F is shown in Fig. 8 for $E_F = -0.7$ (upper panel) and $E_F = -0.3$ (lower panel).

In Sec. II, we have shown that the effective metal-insulator transition for $V < 2t$ is accompanied by a qualitative change of DOS profile as the influence of the lattice comes into play. Duality suggested that these should apply equally to the transitions at $V > 2t$. We note that our arguments in Sec. II near the band edges hold irrespective of V, therefore the band-edge states have the same properties no matter $V > 2t$ or $V < 2t$: the eigenstates are effectively and independently localized within each potential well regardless of the lattices, therefore the quantized and almost degenerate energy levels. However, once the electron density reaches maximum at the potential bottoms, further filling is gradually forced to the neighboring sites, which occurs sequentially in different potential wells according to their respective lattice displacement, changing the spread of the energy eigenvalues and the behavior of DOS.

Note that this transition is unique for $V > 2t$. For $V < 2t$, the shallow potential means that the tunneling between the wells becomes relevant and the gaps in the local integrated DOS between the wells close before the maximum electron filling is ever reached anywhere. The transition is then dominated by the metal-insulator transition. Quite interestingly, the phase transition for $V > 2t$ is an analogy of the metal-insulator transition for $V < 2t$ but with the roles of real space and momentum space interchanged. For $V < 2t$ and energy $|E| < 2t - V$ between the apparent mobility edges, the system is metallic in the sense that the real-space two-point Green's function is long-range and the momentum-space electron density is singular. On the other hand, for $V > 2t$ and energy $|E| < V - 2t$ between the critical points (the insulator* phase in the phase diagram in Fig. 4), the system has singular real-space density and the electron correlation is long-range in Fourier space. See Appendix E for more analytic details. We would like to emphasize that there is no symmetry breaking in either transition. Rather, they are identified by the appearance and disappearance of singularities and changes of physical exponents, yet both are slightly rounded off in the presence of a finite incommensurate Q. Both transitions can be viewed according to the picture used in Sec. II A as a Lifshitz transition in two dimensions projected to one dimension, but along different directions. The duality transformation interchanges the two directions, therefore not surprisingly, it also exchanges the coordinates in which the transition occurs.

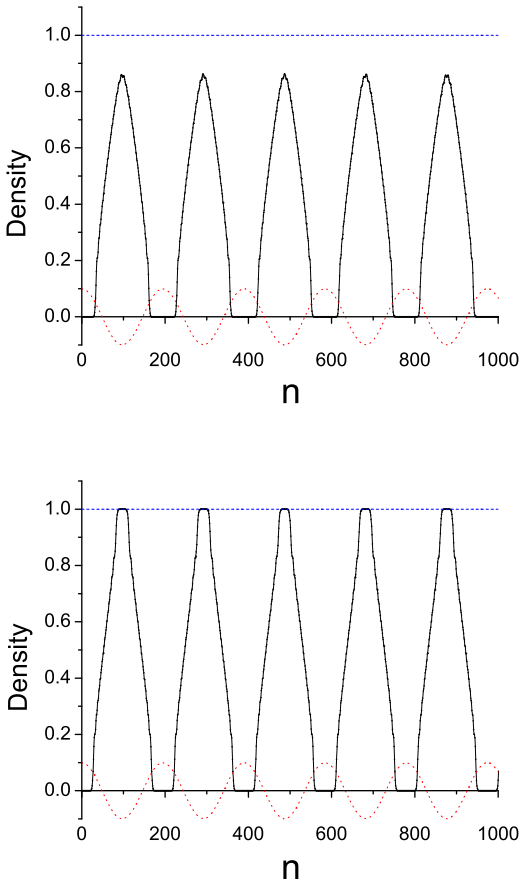

FIG. 8: The real-space electron density of Harper's equation $\int_{-2t-V}^{E_F} dE\,|f_n(E)|^2$ with $t = 1$, $V = 2.5$ and $Q = 1/31$ for all states below the Fermi energy $E_F = -0.7$ (upper panel) and $E_F = -0.3$ (lower panel), respectively. The blue dashed line indicates the maximum electron density allowed - one electron per site. The red dotted curve is an illustration of the incommensurate periodic potential (not to scale).

V. LARGE Q LIMIT

Up until this point, our discussion has focused on the limit in which $Q \ll 2\pi$ is relatively small. For large $Q/2\pi \sim O(1)$, the effective magnetic field is large in the corresponding two-dimensional Hofstadter problem, so the semiclassical theory ceases to be useful. Conversely, we will consider the case in which $V/2t$ is small, so in the original 1D formulation of the problem, we can compute the effects of the incommensurate potential perturbatively and compare with numerical results. We find (consistent with our own earlier findings in Ref. 10) that 1) the lowest orders in the perturbation theory describe Harper's equation satisfactorily so long as $V/2t$ is even mod-

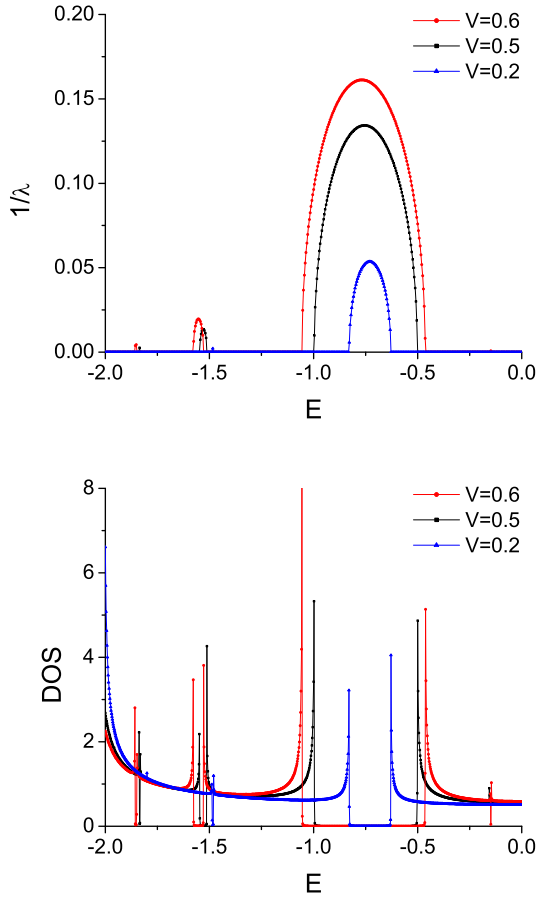

FIG. 9: The inverse localization length (upper panel) and the DOS (lower panel) for Harper's equation with $t = 1$, $V = 0.2, 0.5, 0.6$ and a large $Q = 2\pi \cdot (\sqrt{5}-1)/2$ over the energy range $E \in [-2, 0]$. Due to particle-hole symmetry, only the $E < 0$ half is shown. The peaks in the DOS correspond to the van Hove singularities.

erately small, and 2) all states are de-localized and form a continuous spectrum separated by the gaps, consistent with previous expectations.

In the perturbation theory, we begin with a nearest-neighbor tight-binding model of a one-dimensional chain with energy dispersion $\epsilon_k = 2t\cos(k)$, and then consider the gaps induced by the lowest order scattering from the incommensurate potential. More specifically, the nth order scattering generates an off-diagonal mass term between momentum k and $k + nQ$, resulting in a gap of size $\sim V^n/W^{n-1}$ centering on energy $E_n = \epsilon_k = \epsilon_{k+nQ} = \pm 2\cos(nQ/2)$. The DOS vanishes in the gap and the localization length is finite; between the gaps the spectrum is continuous, and the localization length is infinite.

To check these conclusions, we numerically compute the inverse localization length and DOS of Harper's equation with a large Q. One example is shown in Fig. 9 with hopping amplitude $t = 1$, potential amplitudes $V = 0.2,\ 0.5$, and 0.6 respectively, and wave vector (favored in much of the literature) $Q = 2\pi \cdot (\sqrt{5}-1)/2$. A series of gaps are clearly observed, and the inverse localization length is zero everywhere except inside the gaps. We note that the centers of the gaps from the first three orders of perturbation $E_1 = \pm 2\cos(Q/2) = \pm 0.725$, $E_2 = \pm 2\cos(Q) = \pm 1.475$ and $E_3 = \pm 2\cos(3Q/2) = \pm 1.793$ and their corresponding sizes are remarkably consistent with our numerical results in Fig. 9. In addition, Van Hove singularities in the DOS are clearly seen in the DOS on the band edges. These conclusions are straightforward to generalize to other Q.

One major distinction between the incommensurate and commensurate potentials is that in the former case there is an unending cascade of higher order gaps while in the latter case new gaps are not generated beyond the order of perturbation theory corresponding to the commensurability[10]. So why can we expect a finite-order perturbation theory to work for Harper's equation? Heuristically, the obtained gaps as well as the resulting inverse localization length are exponentially small ($\sim (V/2t)^n$) which eventually results in gaps that are unobservable given a finite energy resolution δ and system size L. In general, for any given level of desired energy resolution δ and system size L there is no essential distinction between the incommensurate problem and a suitable high order commensurate approximant.

VI. CONCLUSION AND DISCUSSIONS

We have revisited important properties of Harper's equation. This problem exhibits many extraordinary features, valid as matters of principle, if studied with infinite precision, *i.e.* assuming infinite energy resolution, perfect periodicity of the incommensurate potential, and no higher harmonics to the potential. This complexity includes conclusions concerning the non-existence of a true mobility edge which is a consequence of an exact self-duality, and a self-similar structure of the spectrum. However, if there is a small parameter, from a physical perspective, in which there is always a finite limit with which physical quantities can be controlled, *exponentially small* effects are physically negligible.

For $Q \ll 2\pi$, the previous conclusion that there is a single metal insulator transition at $V = 2t$ for arbitrary energy E holds in the strict sense. However, in the more physical sense in which a finite energy resolution is present due to disorder, finite temperature, system size limit etc., we find two "effective" mobility edges at $\pm E_c = 2t - V$ for $V < 2t$ and $Q \ll 2\pi$; the states near the band edges are for most physical purposes localized even for a weak incommensurate potential. Moreover, we have discovered a crossover at $\pm E_c = V - 2t$ for $V > 2t$ and $Q \ll 2\pi$ that is dual to the metal insulator transition and characterized by the emergence of a real-space Fermi surface.

Through both perturbative methods and equivalent modeling, we have self-consistently re-established the properties of the various phases of Harper's equation. We note that for small $Q \ll 2\pi$, the two-dimensional Hofstadter problem has a quantized Hall conductance of $\sigma_{xy} = ne^2/h$ if we fill n discrete energy levels near the band edges, so that n electrons will be transported along the $\hat{x}$ direction in each cycle of $k_y \in [0, 2\pi]$.

On the other hand, in the one-dimensional representation of Harper's equation, k_y is the initial phase of the incommensurate potential, which is adiabatically shifted by exactly one period in each cycle of k_y. Since there are n electrons localized in each period of the potential for the limit we are considering, it is straightforward to see that n electrons are pumped from one end of the chain to the other. Such adiabatic pumping process in quasiperiodic systems has been previously studied in Ref. 12,13. Similar argument also implies a connection of Harper's equation with certain commensurate wave vectors to three-dimensional Weyl semi-metal[14].

The methods and conclusions in the main text can be generalized straightforwardly to models with further neighbor hopping or more complex potentials[10]. One interesting example is the 'correlated disorder' of the form $V\cos(Qx^\gamma)$ with an incommensurate wave vector Q. For $\gamma = 1$, the potential is reduced to Harper's equation. Based on a different technique[15], mobility edges have been identified for $\gamma < 1$ and the states are fully localized for $\gamma > 1$.

We acknowledge insightful discussions with Boris Spivak, Pavan Hosur, Xiao-liang Qi, Andre Broido, Sankar Das Sarma, and Persi Diaconis. YZ is supported by the Stanford Institute for Theoretical Physics, DB is supported by the National Science Foundation Graduate Research Fellowship under Grant No. DGE-114747, CMJ is supported by the David and Lucile Packard foundation and National Science Foundation under Grant No. NSF PHY11-25915, AM is supported by DOE Office of Basic Energy Sciences under contract No. DEAC02-76SF00515(AM), and SAK is supported in part by the NSF under grant DMR-1265593 at Stanford. YZ and CMJ also thanks the hospitality of KITP where part of this work is completed and support in part from KITP by the National Science Foundation under Grant No. NSF PHY11-25915.

[1] S. Aubry and C. André, Proc. Israel Physical Society, ed. C.G. Kuper 3, Page 133 (1979).
[2] J.B. Sokoloff, Physics Reports (Review Section of Physics Letters) 126. No. 4, Page 189 (1985).
[3] A. Y. Gordon, S. Jitomirskaya, Y. Last, B. Simon, Acta Mathematica, 178, Issue 2, Page 169 (1997).
[4] Artur Avila, Svetlana Jitomirskaya, Annals of Mathematics, Vol. 170, Issue 1, Page 303 (2009).
[5] Yoram Last, Sturm-Liouville Theory: Past and Present, Page 99 (2005).
[6] Giacomo Roati, Chiara D'Errico, Leonardo Fallani, Marco Fattori, Chiara Fort, Matteo Zaccanti, Giovanni Modugno, Michele Modugno, and Massimo Inguscio, Nature 453, 895 (2008).
[7] Hisashi Hiramoto, Mahito Kohmoto, International Journal of Modern Physics B, Vol. 6, No 3&4, Page 281 (1992).
[8] Svetlana Ya. Jitomirskaya, Annals of Mathematics 150, 1159 (1999).
[9] J. Biddle and S. Das Sarma, Phys. Rev. Lett. 104, 070601 (2010); J. Biddle, D. J. Priour, Jr., B. Wang, and S. Das Sarma, Phys. Rev. B 83, 075105 (2011); Sriram Ganeshan, S. Das Sarma, eprint-arXiv:1411.7375.
[10] Yi Zhang, Akash V. Maharaj, Steven Kivelson, eprint-arXiv: 1410.5108.
[11] R G Chambers, Proc. Phys. Soc. 88 701 (1966).
[12] D. J. Thouless, Phys. Rev. B 27, 6083 (1983).
[13] Yaacov E. Kraus, Yoav Lahini, Zohar Ringel, Mor Verbin, and Oded Zilberberg, Phys. Rev. Lett. 109, 106402 (2012).
[14] Sriram Ganeshan, Kai Sun, and S. Das Sarma, Phys. Rev. Lett. 110, 180403 (2013); Sriram Ganeshan, S. Das Sarma, eprint-arXiv:1405.4866.
[15] F. M. Izrailev and A. A. Krokhin, Phys. Rev. Lett. 82, 4062 (2014).
[16] B. Simon, Almost periodic Schrodinger operators: A review, Adv. Appl. Math. 3, 463 (1982).
[17] J. Avron and B. Simon, Almost periodic Schrodinger operators II: The integrated density of states, Duke Math. J. 50, 369 (1983).
[18] The inverse is *not* true according to Fig. 2.

Appendix A: The accuracy of θ independence in Harper's equation

In this appendix, we discuss the applicability of physical quantities' θ independence. Mathematically, it was proven that the spectrum of the almost Mathieu equation (Harper's equation) is independent of the choices of θ in the thermodynamic limit and when $Q/2\pi$ is indeed irrational[16,17]. Here we offer a heuristic physical argument.

To start with, we consider an intensive physical quantity $A_l(\theta)$ for a one-dimensional system with finite size $l \gg 1$, where exists in general a sizeable θ dependence. For a larger system size $L = nl$, since the interfaces are negligibly small in comparison with the bulk, we may safely separate the measurement into various smaller components each with length l but different phases $\theta_m = \theta + (m-1)Ql(\mathrm{mod}2\pi)$: $A_{L=nl}(\theta) = \frac{1}{n}\sum_m A_l(\theta_m)$, therefore the θ dependence is averaged out over many different θ_m's. We may then repeat the procedure for even larger system sizes, and in each step the θ dependence scales down. This suggests that the θ dependence is inverse proportionally suppressed as the total system size L. Similar argument works for extensive physical quantities $A_{L=nl}(\theta) = \sum_m A_l(\theta_m)$, which receives just an additional factor of the total system size L.

It is straightforward to see that this argument is valid for the DOS ρ (per site), since the electron density (per site) is extensive (intensive). On the other hand, we show in the following that the correct self-averaging quantity for the localization is the inverse localization length $1/\lambda$.

The localization length is defined in terms of the Green's function G by $G(1, l; \theta) \propto \exp(-l/\lambda_l(\theta))$. Therefore, for a larger system $L = nl$:

$$\begin{aligned} G(1, L; \theta) &\propto \prod_m G(ml - l + 1, ml; \theta) \\ &\propto \prod_m G(1, l; \theta_m) \propto \exp(-\sum_m l/\lambda_l(\theta_m)) \end{aligned} \quad \text{(A1)}$$

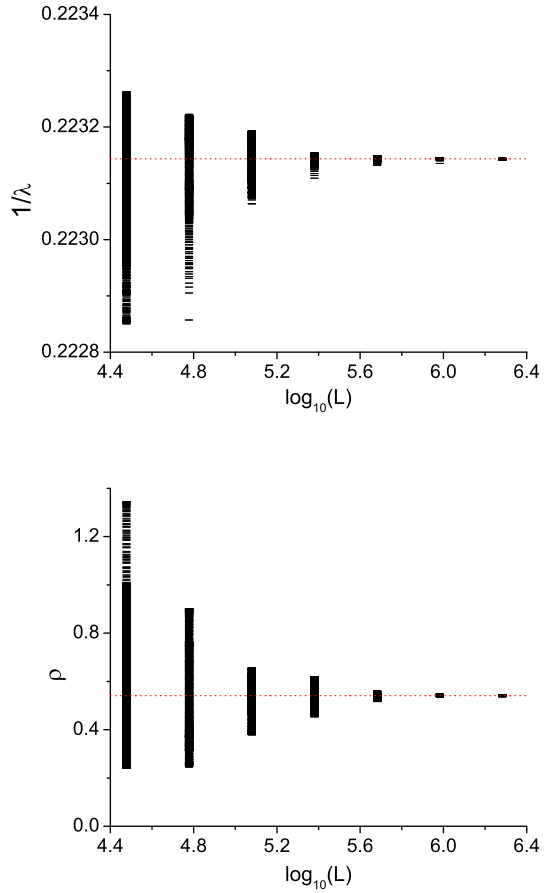

FIG. 10: The system size effect of the spectrum dependence on different choices of θ of the inverse localization length $1/\lambda$ (upper panel) and the DOS ρ (lower panel) of Harper's equation with $t = 1$, $V = 2.5$, $Q = 1/31$ and $E = -0.3$. The red dotted line is the average value over the spectrum for the largest system size.

Comparing this with $G(1, L; \theta) \propto \exp(-L/\lambda_L(\theta))$, we have on the order $O(L)$:

$$\begin{aligned} -L/\lambda_L(\theta) &\approx -\sum_m l/\lambda_l(\theta_m) \\ 1/\lambda_L(\theta) &\approx \frac{1}{n}\sum_m 1/\lambda_l(\theta_m) \end{aligned} \tag{A2}$$

We illustrate in Fig. 10 the system size effect of the spectrum dependence of the inverse localization length $1/\lambda$ and the DOS ρ on different choices of θ. For the system sizes we study in the main text, the θ dependence has been suppressed well enough.

Appendix B: Beyond the free-electron approximation near the band edges

In Sec. II, we have shown that by expanding the energy dispersion ϵ_k to the quadratic order, the free-electron approximation is fairly consistent with numerical results on the DOS near the band edges. In this appendix, we show that the consistency can be made better over a wider range of energy by taking into account the quartic order terms in the expansion:

$$\begin{aligned} H &= -2\cos k - V\cos Qx \\ &\approx -2 - V + k^2 + VQ^2x^2/2 - \frac{1}{24}\left(2k^4 + VQ^4x^4\right) \end{aligned} \tag{B1}$$

where we use the one-dimensional representation and set $t = 1$ and the origin of the coordinate at the potential minimum for simplicity.

Let's define the bosonic ladder operators $a^\dagger|n\rangle = \sqrt{n+1}\,|n+1\rangle$, $a|n\rangle = \sqrt{n}\,|n-1\rangle$ and $a^\dagger a|n\rangle = n|n\rangle$, with which:

$$\begin{aligned} k &= \frac{i\sqrt{\omega}}{2}\left(a^\dagger - a\right) \\ x &= \frac{1}{\sqrt{\omega}}\left(a^\dagger + a\right) \end{aligned} \tag{B2}$$

the canonical commutation relations are preserved. Here $\omega = Q\sqrt{2V}$.

As a consistency check, we first consider the quadratic order:

$$\begin{aligned} H^{(2)} &= k^2 + \omega^2x^2/4 = \frac{\omega}{4}\left[\left(a^\dagger + a\right)^2 - \left(a^\dagger - a\right)^2\right] \\ &= \frac{\omega}{2}\left(a^\dagger a + aa^\dagger\right) = \omega\,(n + 1/2) \end{aligned} \tag{B3}$$

which is diagonal in the $|n\rangle$ representation and has equally spaced energy levels. This is the harmonic oscillator.

We can generalize the expression in terms of the ladder operators to the quartic order:

$$\begin{aligned} H^{(4)} &= -\frac{1}{24}\left(2k^4 + VQ^4x^4\right) \\ &= -\frac{\omega^2}{96}\left[\frac{1}{2}\left(a^\dagger - a\right)^4 + \frac{1}{V}\left(a^\dagger + a\right)^4\right] \\ &= -\frac{\omega^2}{96}\left[\left(\frac{1}{2} + \frac{1}{V}\right)a^\dagger a^\dagger a^\dagger a^\dagger - (4n+6)\left(\frac{1}{2} - \frac{1}{V}\right)a^\dagger a^\dagger + \text{H.c.}\right. \\ &+ \left.\left(6n^2 + 6n + 3\right)\left(\frac{1}{2} + \frac{1}{V}\right)\right] \end{aligned} \tag{B4}$$

which now has off-diagonal components. Still, for the lowest energy levels we can get a sound approximation with a reasonable up-limit for n and exact diagonalize the Hamiltonian in the $|n\rangle$ representation. The results for $V = 1.6$ and $Q = 1/31$ are shown in the blue marks in Fig. 5.

It is straightforward to generalize to higher order expansions.

Appendix C: The tunneling amplitude from WKB approximation

To make a more quantitative estimate of the tunneling amplitude between the neighboring wells t_{eff} in a slowly varying

potential $V\cos(Qx)$, we generalize the canonical WKB approximation to the current dispersion relation:

$$\begin{aligned} 2t\cos\left[k\left(x\right)\right] &- V\cos\left(Qx\right)=E \\ t\left[e^{\kappa(x)}+e^{-\kappa(x)}\right] &= -V\cos\left(Qx\right)-E \\ e^{\pm\kappa(x)} &= -E/2t-\left(V/2t\right)\cos\left(Qx\right) \\ &\pm \sqrt{\left[E/2t+\left(V/2t\right)\cos\left(Qx\right)\right]^{2}-1} \end{aligned} \tag{C1}$$

where the energy E is near the lower band edge and $x \in [0, 2\pi/Q]$ labels the sites between the neighboring wells. Inside the barrier, the wavefunction decays as $e^{-\kappa(x)}$ where $\kappa = ik$ is the imaginary momentum. The tunneling amplitude across all sites among the barrier is

$$\begin{aligned} t_{\text{eff}} \propto \prod_{x} e^{-\kappa(x)} \propto \exp -\sum_{x} \log\{-E/2t \\ -\left(V/2t\right)\cos\left(Qx\right)+\sqrt{\left[E/2t+\left(V/2t\right)\cos\left(Qx\right)\right]^{2}-1}\Big\} \end{aligned} \tag{C2}$$

Replacing the summation with the integral $\int_0^{2\pi/Q} dx$, it is straightforward to see that $t_{\text{eff}} \propto \exp\left[-(2\pi\alpha/Q)\right]$ is exponentially suppressed by the distance $2\pi/Q$ between the potential wells, where

$$\begin{aligned} \alpha = \frac{1}{2\pi}\int_{0}^{2\pi} \log\Big\{ \sqrt{\left[E/2t+\left(V/2t\right)\cos\left(y\right)\right]^{2}-1} \\ -E/2t-\left(V/2t\right)\cos\left(y\right)\Big\}\,dy \end{aligned} \tag{C3}$$

is an increasing function of $V/2t$, since a higher barrier tends to reduce the tunneling amplitude. At the band bottom $E = -2t - V$, the dependence of t_{eff} on $V/2t$ and Q is qualitatively consistent with Eq. 15 from simple variational analysis.

Appendix D: Application to metal-insulator transition of generalized Harper's equation

It is straightforward to generalize Harper's equation to include further neighbor hoppings and higher harmonic components in the incommensurate potential:

$$t\sum_{n'} a_{n'-n} f_{n'} + V f_n \sum_{m} b_m \exp\left(iQm\cdot n\right) = E f_n \tag{D1}$$

where a_n and b_m are given parameters and Q is an incommensurate wave vector. In this appendix, we briefly discuss locating the metal-insulator transition separating the insulating phase for large V and metallic phase for small V in the $Q/2\pi \ll 1$ limit from a two-dimensional Hofstadter problem perspective.

The generalized Harper's equation in Eq. D1 is equivalent to a two-dimensional lattice problem with dispersion $\epsilon(\vec{k}) = t\sum_n a_n \exp\left(ik_x n\right) + V\sum_m b_m \exp\left(ik_y m\right)$ in a magnetic field $B_z = Q/2\pi$. According to Sec. II, the states at energy E are fully de-localized (localized) if the Fermi surface defined by $\epsilon(\vec{k}) = E$ is open along the $\hat{y}$ direction ($\hat{x}$ direction). Yet, as we have shown in Sec. III, the *true* metal-insulator transition is determined by the quantum tunnelings across the $\hat{x}$ and $\hat{y}$ directions when the Fermi surface is closed:

$$\begin{aligned} \tilde{t}_x &= \exp\left(-\frac{1}{2\pi}\int_0^{2\pi}\left|Imk_y(k_x)\right|dk_x\right) \\ \tilde{t}_y &= \exp\left(-\frac{1}{2\pi}\int_0^{2\pi}\left|Imk_x(k_y)\right|dk_y\right) \end{aligned} \tag{D2}$$

where $k_x(k_y)$ and $k_y(k_x)$ are solutions of the dispersion $\epsilon(\vec{k}) = E$ for a given k_y and k_x, respectively. It is also straightforward to see that $\tilde{t}_y$ and $\tilde{t}_x$ are related to the $1/Q$ coefficients in the one-dimensional tunneling amplitude between the neighboring potential wells in the original Harper's equation and dual Harper's equation, respectively. We have listed some examples as follows:

Generalized Harper's equations with implicit self-duality: In Ref. 9, mobility edges have been identified for the following generalized Harper's equations:

$$\begin{aligned} t\left(u_{n-1}+u_{n+1}\right)+V_n u_n = E u_n \\ V_n = 2V\frac{\cos\left(Qn+\phi\right)}{1-r\cos\left(Qn+\phi\right)} \end{aligned} \tag{D3}$$

which can be mapped to an equivalent non-interacting two-dimensional lattice model in the presence of an incommensurate magnetic field of $B_z = Q/2\pi$ with dispersion:

$$\begin{aligned} 2t\cos k_x + 2V\frac{\cos k_y}{1-r\cos k_y} &= E \\ 2t\cos k_x\left(1-r\cos k_y\right)+2V\cos k_y &= E\left(1-r\cos k_y\right) \\ -2rt\cos k_x\cos k_y + 2t\cos k_x &+ \left(2V+rE\right)\cos k_y = E \end{aligned} \tag{D4}$$

It is straightforward to see that for $2V + rE > 2t$ ($2V + rE < 2t$) the constant energy contour at E is elongated along the $\hat{x}$ direction ($\hat{y}$ direction), $\tilde{t}_x$ ($\tilde{t}_y$) is dominant and the model is localized (de-localized) along the initial $\hat{x}$ direction. Clearly, there is a mobility edge at $E = 2\left(t - V\right)/r$, where the Fermi surface is symmetric under $k_x \leftrightarrow k_y$ and $\tilde{t}_x = \tilde{t}_y$. This result is fully consistent with the conclusions in Ref. 9. It is also simple to check the consistency of our argument with the other model in Ref. 9:

$$V_n = 2V\left[1-\cos\left(Qn+\phi\right)\right]/\left[1+r\cos\left(Qn+\phi\right)\right] \tag{D5}$$

Similar self-duality and mobility edge arguments can be generalized to two-dimensional incommensurate Hofstadter problems with dispersion of the following form:

$$h\left(\cos k_x\right)+\frac{a+b\cdot h\left(\cos k_y\right)}{c+h\left(\cos k_y\right)} = E \tag{D6}$$

where $h(t)$ is a power series of t and a, b, c are parameters. The mobility edge is at $E = b - c$.

Generalized Harper's equation with nearest and next-nearest neighbor hopping: we don't always have the luxury

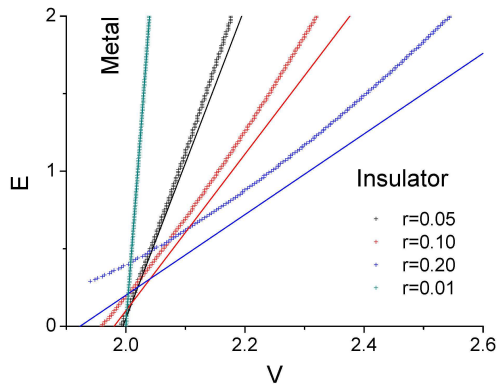

FIG. 11: Phase diagram and mobility edge of generalized Harper's equation in Eq. D7 for various next-nearest and nearest neighbor hopping amplitude ratio r. The results are obtained through calculations of Eq. D2. The solid lines are the exact mobility edges[9] for the approximants with hopping amplitudes $t_n = r^{n-1}t$.

of symmetry for the determination of the relative strength of $\tilde{t}_y$ and $\tilde{t}_x$ in a generic dispersion $\epsilon(\vec{k})$, therefore, we need to calculate $\tilde{t}_y$ and $\tilde{t}_x$ using Eq. D2. One simple example is:

$$t\left[(u_{n-1}+u_{n+1})+r\left(u_{n-2}+u_{n+2}\right)\right]+V\cos(Qn)u_n = Eu_n \quad \text{(D7)}$$

where r is the ratio of the next-nearest neighbor to the nearest neighbor hopping amplitude. We numerically calculate $\tilde{t}_y$ and $\tilde{t}_x$ from the dispersion relation of the corresponding two-dimensional Hofstadter problem $\epsilon(\vec{k}) = t\left(\cos k_x + r\cos 2k_x\right) + V\cos k_y$, and the metal-insulator phase boundaries for various r is shown in Fig. 11. In addition, the exact locations of the mobility edges[9] for approximants of Eq. D7 with hopping amplitudes $t_n = r^{n-1}t$, $n = 1, 2, \cdots$ are shown for comparative purposes.

Appendix E: Characteristic correlations of a real-space Fermi surface

From the duality transformation in Eq. 3 we obtain:

$$\left\langle c_n^\dagger c_0\right\rangle = \frac{1}{L}\sum_{m,m'=1}^{L}\tilde{c}_m^\dagger\tilde{c}_{m'}\exp\left(imnQ+i\theta m-i\theta m'\right) \quad \text{(E1)}$$

where $\tilde{c}$ is the electron operator for the dual Harper's equation with $V > 2t$. We take advantage of the fact that for a quasiperiodic system the correlations are independent of the choices of θ:

$$\begin{aligned}\left\langle c_n^\dagger c_0\right\rangle &= \frac{1}{2\pi L}\sum_{m,m'=1}^{L}\tilde{c}_m^\dagger\tilde{c}_{m'}\int d\theta\exp\left(imnQ+i\theta m-i\theta m'\right)\\ &= \frac{1}{L}\sum_{m,m'}\tilde{c}_m^\dagger\tilde{c}_{m'}\exp\left(imnQ\right)\delta_{mm'}\\ &= \frac{1}{L}\sum_{m}\tilde{c}_m^\dagger\tilde{c}_m\exp\left(imnQ\right)=\tilde{\rho}\left(nQ\right) \quad \text{(E2)}\end{aligned}$$

where $\tilde{\rho}(nQ)$ is the Fourier transform of the electron density of the dual model.

In Sec. II, we have shown that for Harper's equation with $V < 2t$ and $Q \ll 2\pi$, the electron states near the band edge are effectively localized in the physical limit with finite energy resolution δ, and the Green's function $\left\langle c_n^\dagger c_0\right\rangle$ is exponentially suppressed as a function of n; otherwise, near the band center between the mobility edges, $\left\langle c_n^\dagger c_0\right\rangle$ is finite for all n. According to Eq. E2, for the dual Harper's equation with $V > 2t$, the Fourier transform of the density $\tilde{\rho}\left(nQ\right)$ near the band edge is order $\sim O(1)$ when n is small, since the electron density has an induced charge density wave with wave vector Q; however, at large $n \to \infty$, $\tilde{\rho}\left(nQ\right) \to 0$ is suppressed exponentially. In contrast, around the band center within the energy range $E \in (2t - V, V - 2t)$, the emergence of real-space electron density singularities (see our conclusions in Sec. IV) allows the Fourier components $\rho(nQ)$ to be finite for all $n \in \mathbb{Z}$.